**PREPARED FOR THE U.S. DEPARTMENT OF ENERGY,
UNDER CONTRACT DE-AC02-76CH03073**

PPPL-3528
UC-70

PPPL-3528

Signal Propagation in Collisional Plasma with Negative Ions

by

I. Kaganovich, S.V. Berezhnoi, and C.B. Shin

December 2000

PPPL
PRINCETON PLASMA
PHYSICS LABORATORY

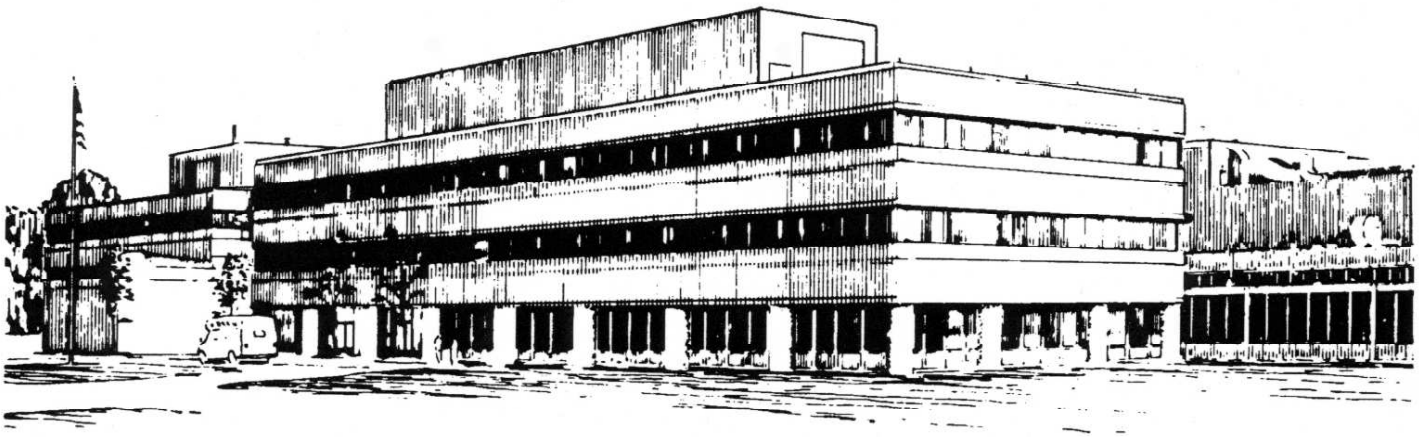

**PRINCETON PLASMA PHYSICS LABORATORY
PRINCETON UNIVERSITY, PRINCETON, NEW JERSEY**

PPPL Reports Disclaimer

This report was prepared as an account of work sponsored by an agency of the United States Government. Neither the United States Government nor any agency thereof, nor any of their employees, makes any warranty, express or implied, or assumes any legal liability or responsibility for the accuracy, completeness, or usefulness of any information, apparatus, product, or process disclosed, or represents that its use would not infringe privately owned rights. Reference herein to any specific commercial product, process, or service by trade name, trademark, manufacturer, or otherwise, does not necessarily constitute or imply its endorsement, recommendation, or favoring by the United States Government or any agency thereof. The views and opinions of authors expressed herein do not necessarily state or reflect those of the United States Government or any agency thereof.

Availability

This report is posted on the U.S. Department of Energy's Princeton Plasma Physics Laboratory Publications and Reports web site in Calendar Year 2000. The home page for PPPL Reports and Publications is: http://www.pppl.gov/pub_report/

DOE and DOE Contractors can obtain copies of this report from:

U.S. Department of Energy
Office of Scientific and Technical Information
DOE Technical Information Services (DTIS)
P.O. Box 62
Oak Ridge, TN 37831

Telephone: (865) 576-8401

Fax: (865) 576-5728

Email: reports@adonis.osti.gov

This report is available to the general public from:

National Technical Information Service
U.S. Department of Commerce
5285 Port Royal Road
Springfield, VA 22161

Telephone: 1-800-553-6847 or
(703) 605-6000

Fax: (703) 321-8547

Internet: http://www.ntis.gov/ordering.htm

Signal propagation in collisional plasma with negative ions

I. Kaganovich[a),1] , S.V. Berezhnoi[b),2] , C.B. Shin[b),3]

[a] Plasma Physics Laboratory, Princeton University, NJ 08543

[b] *Ajou University, Suwon, 442-749, S. Korea*

The transport of charged species in collisional currentless plasmas is traditionally thought of as a diffusion-like process. In this paper, it is demonstrated that, in contrast to two-component plasma, containing electrons and positive ions, the transport of additional ions in multi-species plasmas is not governed by diffusion, rather described by nonlinear convection. As a particular example, plasmas with the presence of negative ions have been studied. The velocity of a small perturbation of negative ions was found analytically and validated by numerical simulation. As a result of nonlinear convection, initially smooth ion density profiles break and form strongly inhomogeneous shock-like fronts. These fronts are different from collisionless shocks and shocks in fully ionized plasma. The structure of the fronts has been found analytically and numerically.

PACS numbers: 52.35 Lv, 52.35Tc, 52.75 Rx

---

[1] e-mail: ikaganov@pppl.gov,

[2] On leave from Physical Technical Department, St. Petersburg State Technical University, 195251, Russia, berezhnoj@phtf.stu.neva.ru

[3] e-mail: cbshin@madang.ajou.ac.kr

I. INTRODUCTION

Discharges in electronegative gases (sixth and seventh group of periodic table) form a large number of negative ions. One of the most important examples of electronegative plasmas is atmospheric electricity. Another example is discharges in halogen gases, typically used in material processing for semiconductor manufacturing [1]. In some applications negative ion beams are preferable than positive ion beams and discharges in electronegative gases are used as a source of negative ions[2]. The ionospheric D-layer [3] is also one of the examples of atmospheric plasma with large percentage of negative ions. Recently large interest was devoted to dusty plasmas, dust particles are negatively charge and can be viewed as large negative ion[4].

We focus on general properties of partially ionized nonstationary collisional plasma transport where the ion mean free path is smaller than the plasma chamber dimensions. Generally transport of charged species in muti-component plasmas is thought to be some sort of ambipolar diffusion [5]. In this paper, it was demonstrated that, in contrast to two-component plasma, containing electrons and positive ions, the transport of additional ions in multi-species plasmas is not governed by diffusion, rather described by nonlinear convection. Ion density discontinuities may form as a result of nonlinear convection and ion density profile break. In this paper we generalize results received in Ref. 6 and 7 for a case of current carrying plasmas. Though the front formation for currentless plasma was already proposed in Ref. 8, this paper lacked rigorous analysis of small signal propagation and good numerical examples, thus, the results were not disseminated in plasma physics community.

The paper is organized in six sections: section II describes the main set of equations; section III considers results of a linear theory of dynamics of small perturbations of negative ions in inhomogeneous partially ionized plasma; section IV generalizes the results of linear theory on the nonlinear case and describes formation of negative ion density discontinuities- fronts; section V is devoted to the front structure; and section VI contains the conclusion and outlook.

II. DESCRIPTION OF THE MODEL

A) System of equations

We assume that the ion mean free path is small compared to the characteristic discharge dimension and examine one-dimensional species transport in a parallel plate geometry. The charged species fluxes in collisional partially ionized plasma are described by a drift-diffusion approximation

$$\Gamma_k = -D_k \frac{\partial n_k}{\partial x} - \mu_k n_k e E ,$$

where D_k and μ_k are the *k*-species diffusion coefficient and mobility, respectively, linked by the Einstein relation $D_k = T_k \mu_k / e$. T_k is the *k*-species temperature. We shall address only currentless plasma with zero net current $j = e(\Gamma_p - \Gamma_n - \Gamma_e) = 0$. Taking into consideration only one positive and one negative ion species with densities (n_p , n_n , respectively), the self-consistent electrostatic field (E) is given [5] by

$$E = \frac{D_p \nabla n_p - D_n \nabla n_n - D_e \nabla n_e}{\mu_p p + \mu_n n + \mu_e n_e} \qquad (1a).$$

Subscripts *p, n*, and *e* correspond to positive ions, negative ions, and electrons, respectively, and $\nabla = \frac{\partial}{\partial x}$. Below we shall consider only the case when the electron density is such that $\mu_e n_e >> \mu_n n, \mu_p p$ and its gradient is not too small ($D_e \nabla n_e >> D_n \nabla n_n, D_p \nabla n_p$); and electrons are described by Boltzmann equilibrium:

$$E = -T_e / e \nabla (\ln n_e), \tag{1b}$$

which gives an explicit relation between electric field and the logarithmic electron density gradient. Even though electron drift flux is larger than ion drift fluxes, the electronegativity n / n_e can be large, since the ratio of mobilities is huge, is of the order of few hundreds. Eq.(1b) for the electric field, along with the continuity equations for negative ion (Eqs.2a) and positive ion number density (Eqs.2b), and the electroneutrality constraint [Debye radius is assumed small, Eqs.(3)], yield a complete system of equations that describes the spatiotemporal evolution of charged species densities, fluxes, and electric field

$$\frac{\partial n_n}{\partial t} - \mu_n \frac{\partial}{\partial x}\left(T_i \frac{\partial n_n}{\partial x} + eEn_n \right) = \nu_{att} n_e - \nu_d n_n - \beta_{ii} n_n n_p , \tag{2a}$$

$$\frac{\partial n_p}{\partial t} - \mu_p \frac{\partial}{\partial x}\left(T_i \frac{\partial n_p}{\partial x} - eEn_p \right) = \nu_{ioniz} n_e - \beta_{ii} n_n n_p , \tag{2b}$$

$$n_e = n_p - n_n . \tag{3}$$

In the above equations, β_{ii} is the ion-ion recombination rate coefficient, ν_{ioniz} , ν_{att}, and ν_d are the ionization, attachment, and detachment frequencies, respectively.

Being focused on general properties of nonlinear transport, we neglected source terms and assumed ion mobilities as constant.

The system (1-3) for positive and negative ion densities can be rewritten in terms of negative ion density and electron density.

$$\frac{\partial n_n}{\partial t} - \frac{\partial}{\partial x}\left(\mu_n T_i \frac{\partial n_n}{\partial x} - u_n n_n \right) = 0 , \tag{4a}$$

$$\frac{\partial n_e}{\partial t} - \frac{\partial}{\partial x}\left(D_{eff} \frac{\partial n_e}{\partial x} \right) - \frac{\partial}{\partial x}\left((\mu_p - \mu_n) T_i \frac{\partial n_n}{\partial x} \right) = 0 , \tag{4b}$$

$$u_n \equiv \frac{\mu_n T_e}{n_e} \frac{\partial n_e}{\partial x} , \tag{5a}$$

$$D_{eff}\left(\frac{n_n}{n_e} \right) = \frac{T_e(\mu_p n_p + \mu_n n_n)}{n_e} + \mu_p T_i , \tag{5b}$$

where u_n is the negative ion drift velocity, D_{eff} is the effective electron diffusion coefficient. The new system of Eqs.(4, 5) is more transparent than the initial system (2), since (4b) has only diffusive term, in contrast to the both, diffusion and drift terms of Eqs.(2a,b).

B) Numerical method

The system of Eqs. (1b, 2, 3) has been solved with finite difference method. The flux-corrected transport technique (FCT) was employed for Eq. (2). The second order FCT method [6] was necessary to use for suppressing numerical diffusion, arising from the convection term.

In the FCT technique the first step is to calculate the initial guess (predictor) at next *(n+1)* step in time (τ) at j-th point in space, chosen on uniform mesh with grid space (*h).*

$$n_j^* = n_j^n - \frac{\tau}{2h}\left(-u_r n_r + u_l n_l \right) + \nu\left(n_{j+1}^n + n_j^n + n_{j-1}^n \right),$$

where $u_r = (u_j^n + u_{j+1}^n)/2$, $u_l = (u_j^n + u_{j-1}^n)/2$, $n_r = (n_j^n + n_{j+1}^n)/2$ $n_l = (n_j^n + n_{j-1}^n)/2$, and $n_j^n \equiv n_n(n\tau, x_j)$, $u_j \equiv u_n(x_j)$, ν is numerical positive diffusion coefficient. The second step is to calculate corrector fluxes

$$f_{j+1/2}^c = sign(\Delta n_{j+1/2}) \max\left\{0, \min\left[\Delta n_{j-1/2} sign(\Delta n_{j+1/2}), \mu\left|\Delta n_{j+1/2}\right|, \Delta n_{j+3/2} sign(\Delta n_{j+1/2})\right]\right\},$$

where $\Delta n_{j+1/2} = n_{j+1}^* - n_j^*$, and coefficient μ determines anti-diffusion. The third step calculates the value of n_j^{n+1} $n_j^{n+1} = n_j^* - f_{j+1/2}^c + f_{j-1/2}^c$.

Ref. 9 recommends the following values for single convection equation $\nu = 1/6 + C^2/3$, $\mu = 1/6 - C^2/6$, where C=uτ/h. However, we found that the optimal choice of the values of μ,ν for system of Eq. (1b, 2, 3) was 0.005, for the best illumination of numerical diffusion and dispersion.

III. SMALL PERTURBATION DYNAMIC

We first study the small signal propagation in unbounded uniform plasma. In gas discharges, ion temperature is a factor of hundred less compared to electron temperature; as a result, ion diffusion may be neglected compared with drift.

The ion and electron density variations δn_α are taken to be of the form $\delta n_\alpha \, exp(-i\omega t + ikx)$. Substitution of charged species variations into (4) results in

$$-i\omega\delta n - \mu_n T_e k^2 \frac{n}{n_e}\delta n_e = 0, \tag{6a}$$

$$-i\omega\delta n_e + D_{eff} k^2 \delta n_e = 0, \tag{6b}$$

$$\delta n_e = \delta n_p - \delta n_n, \tag{6c}$$

There are two modes. The first mode, in which the electron density remains uniform ($\delta n_e = 0$) $\delta n_p = \delta n_n$, does not evolve in time (its slow dissipation is described by the ion diffusion omitted here), and its frequency equals to zero

$$\omega_1 = 0 . \qquad (7a)$$

The second mode evolves with frequency:

$$\omega_2 = -iD_{eff} k^2 . \qquad (7b)$$

This mode corresponds to monotonic decay of a density perturbation with effective diffusion coefficient D_{eff}. Short wavelength modes (large k) decay more rapidly.

The evolution scenario in this case is close to the situation in the pure two component plasma with diffusion coefficient D_{eff}, instead of the ordinary ambipolar coefficient in two-component plasma $D_a \equiv \mu_p T_e$. In the limit of the two-component plasma, negative ion density equals to zero and the effective diffusion coefficient (5b) coincides with ambipolar diffusion coefficient. At large electronegativity, ($n_n/n_e >> 1$) the effective diffusion coefficient (5b) is much greater than the ambipolar diffusion - the presence of the negative ions can strongly enhance the value of D_{eff}. This property strongly influences the evolution of the electronegative plasma profiles, as will be discussed below.

The signal propagation is different, if the inhomogeneity of the background plasma is taken into account, in particular the electron density gradient: $\partial n_e / n_e \partial x \equiv 1/L_e \neq 0$. The derivations are easier to perform in the limit of small scale perturbations $|kL_e| >> 1$. Linearization of system (4) results in a quadratic equation for frequency:

$$\omega^2 + b\omega - c = 0 , \qquad (8a)$$

$$b = -iD_{eff}k^2\ ,\ c = -\mu_p\,\mu_n T_e^2 ik^3\left(\frac{\partial n_e}{n_e \partial x}\right), \tag{8b}$$

small terms of the order of $(1/kL_e)$ were neglected in (8). From the quadratic equation (8a) for frequency it follows that its roots should satisfy $(\omega_1 + \omega_2) = -b\ \ \omega_1\omega_2 = c$. As we shall see $\omega_1 << \omega_2$; and then immediately $\omega_2 \cong -b$ and $\omega_1 \cong -c/b$, in the leading terms of kL_e:

$$\omega_1 = u_{eff}k\ ,\ u_{eff} = \frac{\mu_n\mu_p}{\mu_n n_n + \mu_p n_p}\frac{T_e \partial n_e}{\partial x}. \tag{9a}$$

$$\omega_2 = -iD_{eff}k^2. \tag{9b}$$

The fast diffusive mode (7b) and (9b) $\omega=\omega_2$, remains unchanged. On the other hand, the static mode (7a) $\omega=\omega_1$ converts into a propagating one (9a). In this mode, the signal moves with the velocity $u_{eff} = u_n\,\mu_p n_e/(\mu_n n_n + \mu_p n_p)$ factor $\mu_p n_e/(\mu_n n_n + \mu_p n_p)$ different from the negative ion drift velocity u_n.

The theoretical predictions were verified by numerical modeling. The propagation of the small perturbation is shown in Fig.1 for three different values of electronegativities (n_-/n_e). When electronegativity is small ($n_-/n_e << 1$), u_{eff} coincides with the drift velocity of negative ions $u_{eff} \approx u_n$. In the opposite case, when electronegativity is large ($n_-/n_e >> 1$), u_{eff} is much lower than the drift velocity u, as can be seen in Fig.1. Theoretical calculations for signal speed exactly coincide with results of numerical simulations as demonstrated in Table 1.

IV. NONLINEAR EVOLUTION OF NEGATIVE ION DENSITY PROFILES AND FORMATION OF NEGATIVE ION FRONTS.

As discussed above the speed of negative ion density perturbation depends significantly on negative ion density. As a result different parts of the profile of large perturbations of negative ion density move with different velocity, and nonlinear evolution results in the profile modification. For analysis of the nonlinear evolution of the negative ion density profile, it is convenient to rederive the small signal propagation velocity (9a) in another way. In narrow perturbations of negative ion density, (in the limit $|kL_e|>>1$), the electron density perturbations evolve much faster ($\omega_2>>\omega_1$), and electron density adiabatically adjusts itself to ion density. Consequently, electron flux varies much more slowly than ion flux, and can be assumed to be nearly constant. Using electron flux as slowly varying variable it is convenient to substitute electron gradient $\partial n_e / \partial x$ by electron flux $\Gamma_e = -D_{eff}\partial n_e / \partial x$, Eq.(4a) can be rewritten in the form:

$$\frac{\partial n}{\partial t} + \frac{\partial}{\partial x}(\Gamma_n) = 0, \tag{10a}$$

$$\Gamma_n = -\Gamma_e \frac{\mu_n n}{\mu_n n + \mu_p p}, \tag{10b}$$

small diffusion term was neglected. Making use of slow variation of electron flux, Eq.(10a) reads

$$\frac{\partial n}{\partial t} + u_{eff}(n)\frac{\partial}{\partial x} n = 0, \tag{10c}$$

$$u_{eff} = \frac{\partial \Gamma_n}{\partial n}$$

where the small signal propagation velocity u_{eff} coincides with the previous estimate (9a), but still remains valid for nonlinear perturbations, too. The evolution of nonlinear negative ion density

perturbation is shown in Fig.2. The general theory of nonlinear convection shows[10], that each point of initial profile $n_0(x)$ moves with it's own velocity $u_{eff}(n)$, and the solution of (10c) is $n = n_0(x - u_{eff}(n_0)t)$.

According to the theoretical predictions, in Fig.2 the regions of small negative ion density move faster than regions of large negative ion density. As a result the front of the profile spreads out, and steepening of the back profile leads to profile break and formation of ion density discontinuity- *ion density fronts* (Fig.2). Note that negative ion density fronts are different from gasdynamic shocks, though both originated from nonlinear convection.

V. STRUCTURE OF NEGATIVE ION FRONTS

The analysis of the front structure can be performed similar to the studies of gasdynamic shocks as described in Ref. 10. In the frame moving with the front, electron density and flux is approximately conserved:

$$\tilde{\Gamma}_e = -T_e \frac{(\mu_p p + \mu_n n)}{n_e} \frac{dn_e}{dx} - V n_e , \tag{11}$$

where V is shock velocity, and tilde denote values in the front frame. From the conservation of electron flux and density, it follows, that electron density gradients to the right (+) and to the left (-) of the shock have to satisfy

$$(\mu_p p + \mu_n n) \frac{dn_e}{dx}\bigg|^{+} = (\mu_p p + \mu_n n) \frac{dn_e}{dx}\bigg|^{-} . \tag{12}$$

Similarly negative ion flux is conserved

$$\tilde{\Gamma}_n = \Gamma_n - V n_n , \tag{13a}$$

and

$$V = \frac{\Gamma_n\big|^{+} - \Gamma_n\big|^{-}}{n_n^{+} - n_n^{-}} \tag{14}$$

Substituting expression for Γ_n (10b) in Eq.(14) results in

$$V = -\frac{\mu_p \mu_n n_e \Gamma_e}{\left(\mu_p (n_n + n_e) + \mu_n n_n\right)^{+} \left(\mu_p (n_n + n_e) + \mu_n n_n\right)^{-}} \tag{15a}$$

Finally, after substituting the expression for electron flux we have

$$V = \frac{\mu_p \mu_n T_e \frac{dn_e}{dx}\Big|^{+}}{\left(\mu_p (n_n + n_e) + \mu_n n_n\right)^{-}} = \frac{\mu_p \mu_n T_e \frac{dn_e}{dx}\Big|^{-}}{\left(\mu_p (n + n_e) + \mu_n n\right)^{+}}. \tag{15b}$$

Table 2 demonstrates good agreement of theoretical predictions for the front speed Eq.(15b) and numerically obtained values for the conditions of Fig.2.

In Fig. 3 the electron and negative ion fluxes are depicted. It is seen that electron flux is nearly conserved, whereas negative ion flux changes rapidly in the front, see Fig.3a. Convective flux Γ_n nearly coincides with Vn showing that the whole profile moves with the speed *V*, see Fig.3b. The difference between two fluxes $\tilde{\Gamma}_n = \Gamma_n - Vn_n$ is small, and is associated with the ion diffusion, see Fig.3c.

Inside the front the total flux is conserved, and ion diffusion is balanced by convective flux in the frame moving with the front . Hence, Eq.(13a) takes the form:

$$\tilde{\Gamma}_n = \Gamma_n - Vn_n - \mu_n T_i \frac{\partial n_n}{\partial x}. \tag{13b}$$

Substituting the expression for convective flux Eq. (10b) and front velocity (15b) we find that at the periphery where diffusive flux tends to zero

$$\tilde{\Gamma}_n = -\frac{\mu_n(\mu_p+\mu_n)n_n^+ n_n^- \Gamma_e}{\left(\mu_p(n_n+n_e)+\mu_n n_n\right)^- \left(\mu_p(n_n+n_e)+\mu_n n_n\right)^+}$$

and diffusion flux reads:

$$-\mu_n T_i \frac{dn_n}{dx} = -V(\mu_n+\mu_p)\frac{(n_n^+ - n_n)(n_n - n_n^-)}{\mu_p n_p + \mu_n n_n} \tag{16}$$

Integration of (16) yields front width:

$$L_{front} = \frac{\mu_n T_i}{V} F\left(\frac{n_+}{n_e}, \frac{n_-}{n_e}, \frac{\mu_n}{\mu_p}\right), \tag{17a}$$

$$F\left(\frac{n_+}{n_e}, \frac{n_-}{n_e}, \frac{\mu_n}{\mu_p}\right) = \int_{s_-}^{s_+} \frac{(s+\delta)ds}{(n_+/n_e - s)(s - n_-/n_e)}, \tag{17b}$$

$$s = \frac{n-n_-}{n_e},\ \delta = \frac{\mu_p}{\mu_p+\mu_n} + \frac{n_-}{n_e},\ s_- = \varepsilon\frac{n_+-n_-}{n_e},\ s_+ = (1-\varepsilon)\frac{n_+-n_-}{n_e},$$

where ε is an arbitrary small number. Integration of (17b) yields

$$F\left(\frac{n_n^+}{n_e}, 0, \frac{\mu_n}{\mu_p}\right) = \ln\left(\frac{1-\varepsilon}{\varepsilon}\right)\left(1+\frac{2\delta n_e}{n_n^+}\right)$$

and front width is

$$L_{front} = \frac{\mu_n T_i}{\mu_p T_e \left|\frac{dn_e}{dx}\right|^-} \ln\left(\frac{1-\varepsilon}{\varepsilon}\right)\left(1+\frac{2\delta n_e}{n_n^+}\right)\left(\mu_p(n+n_e)+\mu_n n\right)^+ \tag{17c}$$

In the case of equal ion mobilities, and choosing $\varepsilon = 0.1$ and $n_+ >> n_-$

$$L_{front} = 2.2 L_e \frac{T_i}{T_e}\left(3 + \frac{n_e}{n_n^+} + \frac{n_n^+}{n_e}\right). \tag{17d}$$

For small electronegativity $n_e >> n_+$

$$L_{front} \approx 2.2 L_e \frac{T_i}{T_e} \frac{n_e}{n_{\mathrm{n}}^+},$$

front sheath is reciprocal of the change in density in the front (n_+); small density discontinuities spreads wider similarly to the Burgers' equation [10], (where flux is quadratic function of densty).

In the opposite case of large electronegativity $n_e << n_+$

$$L_{front} \approx 4.4 L_e \frac{T_i}{T_e} \frac{n_{\mathrm{n}}^+}{n_e}$$

sheath width is proportional to the change in density in the front, in contrast to the Burgers' equation.

In the range $1/2 < n_+ / n_e < 1$ front width varies insignificantly and

$$L_{front} \approx 13 L_e \frac{T_i}{T_e}$$

In other words, the width of the front depends upon the ratio of negative ion density and convective flux; for small electronegativity $n_e >> n_+$ this ratio increases, and, in the opposite case of large electronegativity $n_e << n_+$, the ratio decreases with increase of negative ion density - front width changes respectively.

Comparison of theoretical estimates with numerical simulations is presented in Fig.4 and Table 3. In Fig.4b one can see that the front width increases proportionally to ion temperature.

The examples of front formation in practical discharges are collected in review[11].

VI. Conclusions

In the general case of multi-species plasmas the field-driven fluxes of the charged particles are of a complex nature. Assuming a two-component plasma (positive ions and electrons with densities n_p=n_e), and Boltzmann equilibrium for electrons, the drift flux of positive ions is reduced to an effective linear (ambipolar) diffusion flux. If plasma consists of two or more sorts of ions, the flux of any given species of the charged particles depends, in general, not only on its own density gradient, but also on the density gradients of all the other species. For example, the presence of negative ions substantially influences the charged species fluxes. In a plasma containing negative ions (with density n), the drift flux of negative ions is a nonlinear function of densities, $-\mu_n n_n E = \mu_n T_e n_n \partial \ln n_e / \partial x$, and described by convection, with a velocity that depends nonlinearly on electron densities, and via equation for evolution of electron densities depends nonlinearly on the negative ion density also. We show that in inhomogeneous EN plasmas the small-localized perturbation of positive and negative ion density moves with velocity

$$u_{eff} = \frac{\mu_n \mu_p}{\mu_n n_n + \mu_p n_p} T_e \frac{\partial n_e}{\partial x}.$$

Since u_{eff} is a function of negative ion density, the nonlinear evolution of perturbations results in formations of negative ion density discontinuities - negative ion density fronts, analogous to shocks, which are widely known in gasdynamics [10], and collisional multi-species plasmas, carrying dc current, see Ref. 6, 7. Ion density discontinuities forms as a result of nonlinear convection and ion density profile break. In this paper we have generalized the results received in Ref. 6 for a case of currentless plasmas. The width of the negative ion front is found to be proportional to ratio of ion and electron temperatures times electron inhomogeneity scale.

In summary, plasma with negative ions tends to stratify into regions with presence of negative ions and electro-positive plasmas (without negative ions) the boundary between two regions-front-

is narrow and forms as a result of nonlinear convection and negative ion density profile breaking. The fronts is general phenomenon for collisional multi-species plasma and has to be accounted in study of discharge in electronegative gases [11].

Acknowledgment

The helpful comments of Y. Raitses and E. Startsev are greatly appreciated. Authors also thank Profs. R.N. Franklin, A.J. Lichtenberg and L.D. Tsendin for persistent encouragement to accomplish this paper.

The work of I. Kaganovich was funded by the Princeton Plasma Physics Laboratory (University Collaboration Grant), National Science Foundation, Chemical Transport Systems CTS-9713262, and by Alexander von Humboldt Foundation. S. Berezhnoi was supported by Korea Institute of Science & Technology Evaluation and Planning (KISTEP) program 99RE06-016, International Association of European Union, INTAS grant no. 96-0235, and by Russian program in thermonuclear synthesis UTS grant no. 378. Korea Science and Engineering Foundation (KSEF) grant no. 971-1107-018-2 supported the work of C.B. Shin.

References

1 M.A. Lieberman and A.J. Lichtenberg, *Principles of Plasma Discharges and Materials Processing* (Wiley, NY 1994).

2 M Hopkins and K Mellon, Phys. Rev. Lett. **67**, 449 (1991).

3 W Swider, Ionospheric Modeling, (Birkhauser Verlag, Basel, 1988) p.320.

4 V.N. Tsytovich, Comments on Plasma Physics & Controlled Fusion, **1**(2), part C, 41 (1999)

5 H Massey, Negative ions, (Cambridge University Press, Cambridge, 1976, 3rd ed.), p. 741

6 A.P.Dmitriev, V.A. Rozhansky, L.D.Tsendin. Sov.Phys. - Uspekhi, **28**, 467 (1985).

7 V.A. Rozhansky, L.D.Tsendin, *Transport phenomena in partially ionized plasma*, (Gordon & Breach, NY, 2000), 320 p. (in Russian - Energoatomizdat, Moscow 1988) p.380

8 I. D. Kaganovich, L. D. Tsendin, Plasma Phys. Reports, **19**, 645 (1993).

9 J.P. Boris and D.L. Brook J. Comput. Phys., **68**, 127 (1987)

10 G. B. Whitham, *Linear and Nonlinear Waves* (NY Wiley, 1974) p.220.

11 I. D. Kaganovich, "Negative ion fronts", to be published in Phys. of Plasmas.

Figure captions:

Table 1

Speed of the signal propagation ($10^{-2}\, u_{eff}$) for the conditions of Fig.1, num. denotes the results of numerical simulations, theory – calculations by Eq.9a

Table 2

The comparison of theoretical predictions for the front speed Eq.15b and numerical result, performed for the conditions of Fig.2

Table 3

The comparison of theoretical predictions for the front width Eq.17d and numerical result, performed for the conditions of Fig.4b. num. corresponds to the width calculated as difference between positions of ion density equal to 0.9 and 0.1 of maximum ($x(n=0.9n_{max})$-$x(n=0.1n_{max})$).

Figure 1

Propagation of small signal for the same unperturbed electron density (n_e =3.7-0.3 x) and different densities of unperturbed plasma negative ions. (a) $n \approx 2.0 n_e$ (n =6-0.3 x), (b) $n \approx n_e$ (n =4-0.3 x), (c) $n = 0$. All variables are dimensionless, normalized on some

reference values, density n/n_0, coordinate *x/L*, time $tL^2/(\mu_n T_e)$. Ion diffusion was neglected, and ion nobilities were taken to be the same $\mu_n = \mu_p$.

Figure 2

Propagation of large perturbation of negative ion density for the conditions of Fig.1, but T_i*=0.001* and n_e *=6.2-3.6x,* initially at *t=0* $n = \frac{N}{a\sqrt{\pi}} \exp\left(-\frac{(x-0.93)^2}{a^2}\right)$, where *a=0.0144*, and total number of negative ions *N=0.476*, and negative ion density profiles are plotted 6 times every 0.25 units of dimensionless time.

Figure 3 depicts the front structure. The same conditions as in Fig.2 at *t=1.* a) Negative ion and electron fluxes, electron and negative ion densities and gradient of electron density, b) convective flux Γ_n and Vn where V is front velocity from Eq. 15), c) minus convective flux in the front frame $-(\Gamma_n - Vn) + (\Gamma_n - Vn)|_-$, and diffusive flux $-\mu_n T_i \frac{\partial n}{\partial x}$.

Figure 4. Propagation of the ion density discontinuity. Ion mobilities are constant. The initial profiles of all species are linear *n(x)= 0.4-0.23x* , n_e*(x)= 0.6-0.24x* , at the right boundary positive ion density was fixed *p(0)=1*, at the left negative ion was constrained initially *n(1)=0.17;* at time equal zero boundary condition at left side was change to *n(1)=0.05* causing ion density wave to propagate to the right. Fig 4a) depicts time evolution of perturbation for T_i*=0.001;* Fig. 4b) shows perturbations of negative ion

density (*n- (0.23-0.18x)*) for three different ion temperatures, T_i= *0.002; 0.006, 0.01*. The width of the back front of signal increases proportionally with $_{Ti}$.

Table 1. a) b) and c). Speed of the signal propagation ($10^{-2}\, u_{eff}$) for the conditions of Fig.1a) b) and c), num. denotes the results of numerical simulations, theory – calculations by Eq.9a.

	a)		b)	
time	u_{eff} , num.	u_{eff}, theory	u_{eff}, num.	u_{eff}, theory
0	1.999	1.991	2.701	2.713
10	1.975	1.978	2.642	2.631
20	1.953	1.950	2.587	2.581
30	1.931	1.933	2.536	2.533

c)

time	u_{eff}, num.	u_{eff}, theory
0	8.058	8.012
2	7.933	7.964
4	7.814	7.801
6	7.703	7.701
8	7.596	7.586
10	7.496	7.501

1

[1] Table 1 Kaganovich et.al.

Table 2. The comparison of theoretical predictions for the front speed Eq.15b and numerical result, performed for the conditions of Fig.2

time	V,num.	V, theory
0.00	0.40	0.40
0.25	0.69	0.68
0.50	0.68	0.67
0.75	0.63	0.62
1.00	0.58	0.58
1.25	0.54	0.54

[2] Table 2 Kaganovich et.al.

Table 3.The comparison of theoretical predictions for the front width (17d) and numerical result, performed for the conditions of Fig.4b. num. corresponds to the width calculated as difference between positions of negative ion density equal to 0.9 and 0.1 of the maximum of density perturbations.

T_i/T_e	L_{front}, num.	L_{front}, theory
0.002	0.058	0.050
0.006	0.14	0.14
0.01	0.22	0.24

[3] Table 3 Kaganovich et.al.

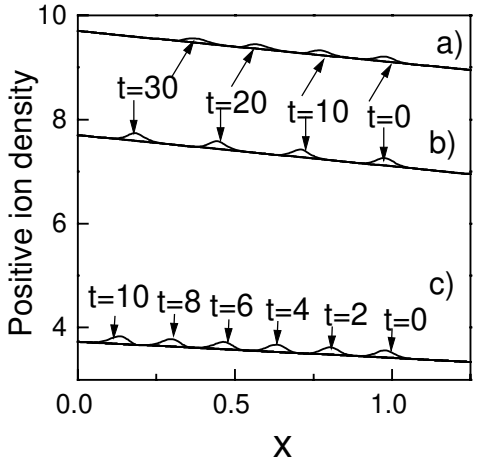

[4] Fig.1 Kaganovich et.al.

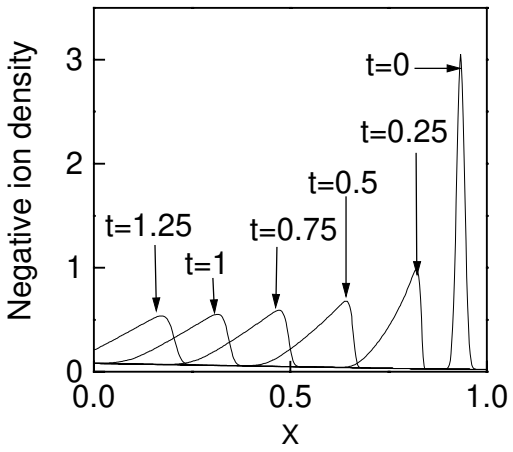

5

[5] Fig.2 Kaganovich et.al.

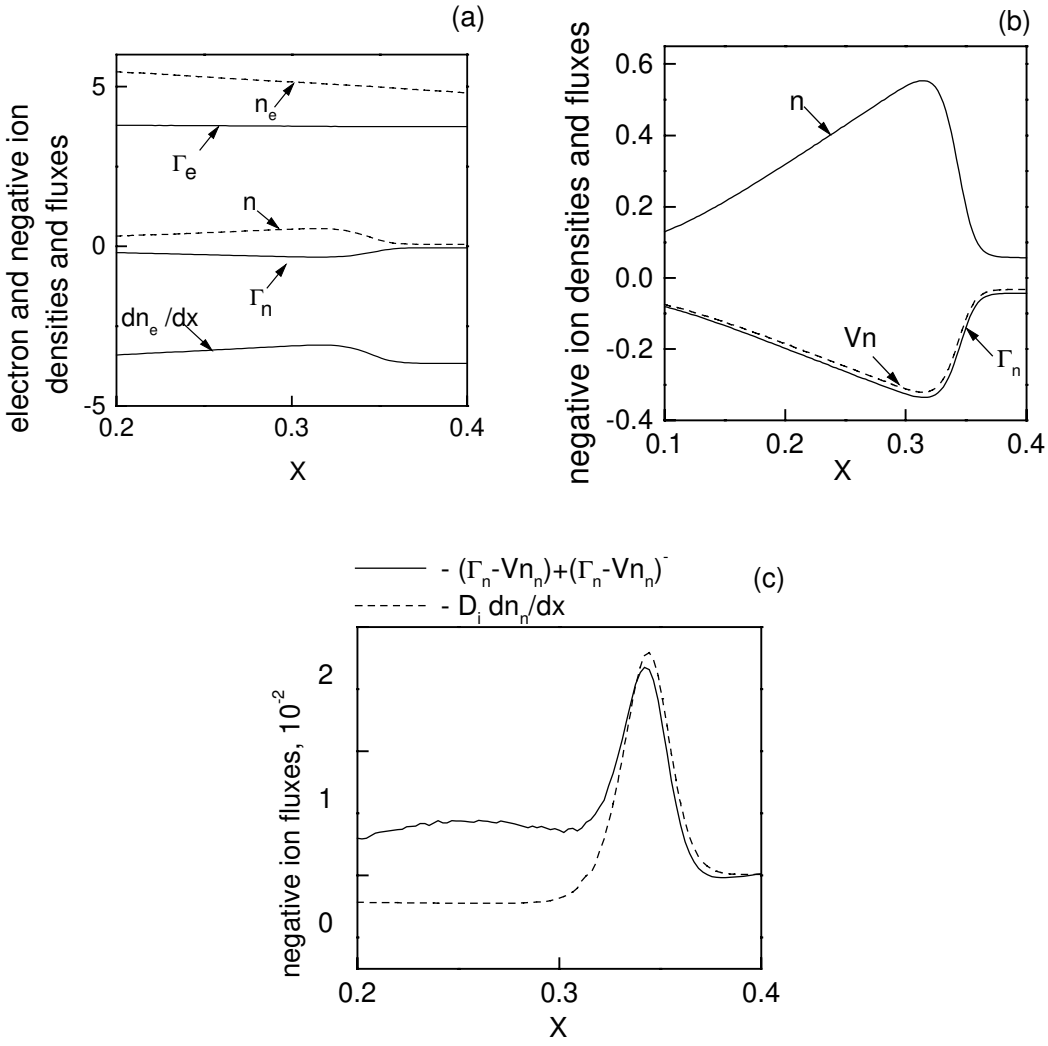

6

[6] Fig.3 Kaganovich et.al.

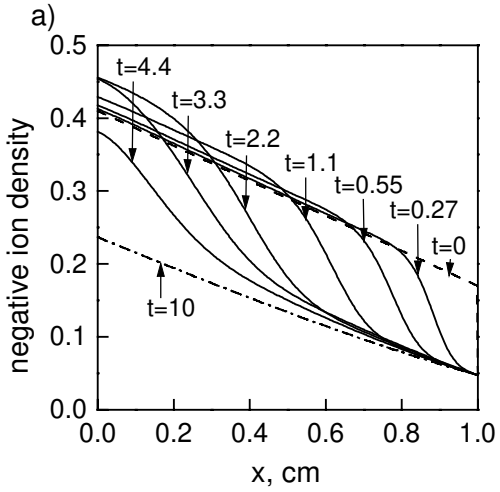

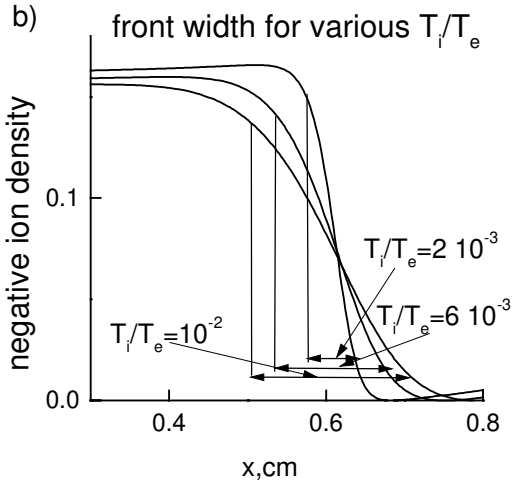

7

[7] Fig.4 Kaganovich et.al.

The Princeton Plasma Physics Laboratory is operated
by Princeton University under contract
with the U.S. Department of Energy.

Information Services
Princeton Plasma Physics Laboratory
P.O. Box 451
Princeton, NJ 08543

Phone: 609-243-2750
Fax: 609-243-2751
e-mail: pppl_info@pppl.gov
Internet Address: http://www.pppl.gov